PIN-FORMED1 and *PINOID* regulate boundary formation and cotyledon development in *Arabidopsis* embryogenesis

Masahiko Furutani[1], Teva Vernoux[2,*], Jan Traas[2], Takehide Kato[1], Masao Tasaka[1] and Mitsuhiro Aida[1,†]

[1]Graduate School of Biological Sciences, Nara Institute of Science and Technology, Nara 630-0101, Japan
[2]INRA, Laboratoire de Biologie Cellulaire, Route de Saint Cyr, 78026 Versailles Cedex, France
*Present address: DCMB Group, Department of Biology, LSRC Building, Research Drive, Box 91000, Duke University, Durham, NC 27708-1000, USA
†Author for correspondence (e-mail: m-aida@bs.naist.jp)

Accepted 20 July 2004

Development 131, 5021-5030
Published by The Company of Biologists 2004
doi:10.1242/dev.01388

Summary

In dicotyledonous plants, two cotyledons are formed at bilaterally symmetric positions in the apical region of the embryo. Single mutations in the *PIN-FORMED1* (*PIN1*) and *PINOID* (*PID*) genes, which mediate auxin-dependent organ formation, moderately disrupt the symmetric patterning of cotyledons. We report that the *pin1 pid* double mutant displays a striking phenotype that completely lacks cotyledons and bilateral symmetry. In the double mutant embryo, the expression domains of *CUP-SHAPED COTYLEDON1* (*CUC1*), *CUC2* and *SHOOT MERISTEMLESS* (*STM*), the functions of which are normally required to repress growth at cotyledon boundaries, expand to the periphery and overlap with a cotyledon-specific marker, *FILAMENTOUS FLOWER*. Elimination of *CUC1*, *CUC2* or *STM* activity leads to recovery of cotyledon growth in the double mutant, suggesting that the negative regulation of these boundary genes by *PIN1* and *PID* is sufficient for primordium growth. We also show that *PID* mRNA is localized mainly to the boundaries of cotyledon primordia and early expression of *PID* mRNA is dependent on *PIN1*. Our results demonstrate the redundant roles of *PIN1* and *PID* in the establishment of bilateral symmetry, as well as in the promotion of cotyledon outgrowth, the latter of which involves the negative regulation of *CUC1*, *CUC2* and *STM* genes, which are boundary-specific downstream effectors.

Key words: Embryogenesis, Cotyledon development, CUC, *PIN1*, *PID*, Auxin, *Arabidopsis thaliana*

Introduction

In dicotyledonous plants, the above-ground part of the seedling exhibits bilateral symmetry, as evidenced by two symmetrically located cotyledons and the shoot apical meristem (SAM) between them. This symmetry can be traced back to early embryogenesis, where two cotyledon primordia start to grow from the apical region of a radially symmetrical globular embryo (Long and Barton, 1998; Bowman and Eshed, 2000; Jürgens, 2001; Aida et al., 2002; Furutani et al., 2003). How plant embryos promote the outgrowth of cotyledon primordia with a bilaterally symmetric pattern has remained an important question and has been studied using physiological or genetic approaches.

Previous studies have indicated that auxin is involved in various patterning processes, including apical patterning during embryogenesis. Auxin displays asymmetric distribution that changes dynamically throughout early embryogenesis and polar auxin transport is important for this distribution (Sabatini et al., 1999; Friml et al., 2002; Benková et al., 2003; Friml et al., 2003). Treatment of embryos with exogenous auxin or polar transport inhibitors causes variable defects in the apical pattern formation, including abnormal positioning or fusion of cotyledons (Liu et al., 1993; Hadfi et al., 1998; Friml et al., 2003). These results suggest that proper auxin distribution is important for the symmetrical positioning of cotyledon primordia and the establishment of cotyledon boundaries.

Genetic studies support the role of auxin in the above-mentioned processes. In *Arabidopsis*, mutations in the *PIN-FORMED1* (*PIN1*), *MONOPTEROS* (*MP*) and *PINOID* (*PID*) genes disrupt the patterning of cotyledons (Okada et al., 1991; Berleth and Jürgens, 1993; Bennett et al., 1995). These mutants are also defective in lateral organ formation from the postembryonic shoot meristem, indicating their significant role in lateral shoot organ development. The *PIN1* gene encodes a member of the putative auxin efflux regulator proteins that promote polar auxin transport (Gälweiler et al., 1998) and is suggested to promote organ formation by regulating auxin distribution (Benková et al., 2003; Reinhardt et al., 2003). The *MP* gene encodes a transcriptional activator that binds in vitro to an auxin-responsive cis-element and is suggested to promote primordium formation by mediating auxin-induced transcriptional activation (Ulmasov et al., 1997a; Hardtke and Berleth, 1998). The *PID* gene encodes a serine/threonine kinase, the transcription of which is induced by exogenous auxin (Christensen et al., 2000; Benjamins et al., 2001). Similar to the *pin1* mutant, the *pid* mutant displays a reduction of polar auxin transport in the stem (Bennett et al., 1995). Moreover, plants overexpressing *PID* exhibit reduced root growth and this phenotype is suppressed by treatment with polar auxin transport inhibitors. These results suggest that *PID* functions as a positive regulator of polar auxin transport (Benjamins et al., 2001).

The expression of *CUP-SHAPED COTYLEDON1* (*CUC1*) and its functionally redundant homolog, *CUC2*, has been analyzed in *pin1* and *mp* mutant embryos (Aida et al., 2002). These genes encode transcription factors of the NAC family, promote cotyledon separation at the boundaries and cause cotyledon fusion when both of them are mutated. Although these two genes are normally expressed in a stripe between cotyledon primordia, *CUC1* expression is expanded to the periphery of the apical region and *CUC2* expression is restricted to the center. The effects of *pin1* or *mp* mutations on *CUC1* and *CUC2* expression are well correlated with the fusion phenotype of *pin1* or *mp* mutants as well as their double mutant combinations with *cuc1* or *cuc2*. These results suggest that *PIN1* and *MP* regulate boundary formation by regulating the *CUC1* and *CUC2* genes. The *SHOOT MERISTEMLESS* (*STM*) gene, a *kn1*-type homeobox gene required for SAM formation and maintenance (Barton and Poethig, 1993; Clark et al., 1996; Endrizzi et al., 1996; Long et al., 1996), also participates in promoting cotyledon separation and its contribution is particularly prominent in the *pin1* mutant background (Aida et al., 2002).

To further investigate the molecular relationship between auxin and apical pattern formation in the *Arabidopsis* embryo, we examined the functions of *PIN1* and *PID* genes in this process. We found that *pin1* and *pid* mutations, when combined in the double mutant, lead to a striking seedling phenotype that is represented by a radially symmetric shape without any cotyledons. This phenotype is associated with the prolonged expansion of *CUC1*, *CUC2* and *STM* expression domains to the periphery of the embryo apex, and contrasts with the mild and transient changes in *CUC1* and *CUC2* expression observed in the *pin1* or *pid* single mutant. Triple and quadruple mutant analysis indicates that the ectopic expression of *CUC1*, *CUC2* and *STM* genes in the *pin1 pid* double mutant is mainly responsible for the growth inhibition of cotyledon primordia. Our results thus demonstrate that the overlapping function of *PIN1* and *PID* is largely responsible for the establishment of bilateral symmetry and cotyledon outgrowth, and that the latter process involves the negative regulation of boundary-specific downstream effectors, the CUC and *STM* genes.

Materials and methods

Plant materials and growth conditions

Arabidopsis thaliana ecotype Lansberg *erecta* (L*er*) was used as the wild type. The following mutant alleles were used: *cuc1-1* (L*er*) (Takada et al., 2001), *cuc2* (L*er*) (Aida et al., 1997), *pin1-3* (L*er*) (Bennett et al., 1995), *pin1-6* [Wassilewskija (WS)] (Vernoux et al., 2000), *pin1-201* [Columbia (Col)], *pid-2* (L*er*) (Christensen et al., 2000), *pid-7.1.2.6* (WS), *pid-3* (Col) (Bennett et al., 1995) and *stm-1* (L*er*) (Barton and Poethig, 1993). *pin1-201* carries a T-DNA insertion at the third intron and is supposed to be null. This allele was obtained from the *Arabidopsis* Biological Resource Center (SALK_047613) (Alonso et al., 2003) and was backcrossed four times to Col wild type prior to any phenotypic analysis and construction of the *pin1 pid* double mutant. The *pid-7.1.2.6* allele contains a substitution that modifies codon 271, creating a stop (Q271 stop) that eliminates approximately one-third of the protein, suggesting that it is a null allele. Plants were grown on soil as previously described (Fukaki et al., 1996), and siliques were collected for analyses of embryo phenotypes and in situ hybridization. Stages of embryogenesis were as defined previously (Jürgens and Mayer, 1994). For analysis of seedling phenotypes, seeds were surface sterilized and germinated on Murashige and Skoog plates, as previously described (Aida et al., 1997).

Construction of double, triple and quadruple mutants

For the construction of the *pin1-3 pid-2* double mutant, plants heterozygous for *pin1-3* were crossed with *pid-2* homozygotes. Among the F2 population, plants homozygous for *pid-2* and heterozygous for *pin1-3* were selected by using PCR primers that detected the mutations and self-fertilized. Among F3 populations, double mutants were selected by PCR-based genotyping or the presence of the novel specific phenotype (see Results). *pin1-6 pid-7.1.2.6* and *pin1-201 pid-3* double mutants also displayed the same phenotype. For the construction of the *pin1 pid cuc1*, *pin1 pid cuc2* or *pin1 pid stm* triple mutants, plants heterozygous for *pin1-3* and homozygous for *pid-2* were crossed with *cuc1-1* homozygous, *cuc2* homozygous or *stm-1* heterozygous plants, respectively. Among the F2 populations, plants homozygous for *cuc1-1* or *cuc2*, or heterozygous for *stm-1* were selected by PCR-based genotyping. These plants were further selected for the heterozygous *pin1-3* and homozygous *pid-2* mutation by PCR, and for the pin-shaped inflorescence phenotype (Bennett et al., 1995). Phenotypes of the triple mutants were examined in the F3 populations and their genotypes were confirmed by PCR. The *STM* and *PIN1* loci were located on chromosome 1 and closely linked. The occurrence frequency of the novel phenotype was 2.4% (n=127), which was nearly identical to that of the *pin1 stm* double mutant, as previously described (Aida et al., 2002). For the construction of the *pin1 pid cuc1 cuc2* quadruple mutant, plants heterozygous for *pin1-3* and homozygous for *pid-2* and *cuc1-1* were crossed with plants heterozygous for *pin1-3* and homozygous for *pid-2* and *cuc2*. Among the F2 populations, plants heterozygous for both *pin1-3* and *cuc1-1*, and homozygous for *cuc2* were selected. Seedling phenotypes of the quadruple mutants were examined in the F3 populations.

Microscopy

For visualization of vasculature, seedlings were cleared as previously described (Aida et al., 1997). Scanning electron microscopy images were obtained as described previously (Aida et al., 1999).

In situ hybridization

In situ hybridization was performed as previously described (Aida et al., 2002). Hybridization was performed at 45°C. Templates for transcription of a *PID* antisense probe were derived from a PCR-amplified 1122 bp fragment corresponding to a region that spanned amino acids 44-417. Probes for the following genes have been reported previously: *ANT* (Long and Barton, 1998), *CUC1* (Takada et al., 2001), *CUC2* (Aida et al., 1999), *FIL* (Sawa et al., 1999) and *STM* (Long et al., 1996). As controls, we confirmed the expression patterns of *FIL*, *PID*, *CUC1* and *CUC2* genes in wild type. For any of these probes, we detected aberrant expression patterns (expanded or reduced) in fewer than 5% of the embryos (three out of 88 for *FIL*; four of 104 for *PID*; six of 113 for *CUC1*; and six of 132 for *CUC2*).

β-Glucuronidase (GUS) GUS staining

To detect GUS activity, embryos were stained with a solution described previously (Takada et al., 2001) at 37°C for 45 minutes. Stained embryos were dehydrated in a graded ethanol series (30, 50, 70, 90 and 100%) for 15 minutes each. Rehydration in a graded ethanol series (90, 70, 50, and 30%) was performed for 15 minutes each before observation.

Auxin treatment

Plants were grown under constant white light exposure until several siliques started to develop (~3 weeks). All developing siliques were cut off before auxin treatment. The plants were subsequently sprayed with a heavy mist of 10 μM 2,4-dichlorophenoxy-acetic acid with 0.01% Silwet L-77. Mock treatments were performed with distilled

water containing 0.01% Silwet L-77. Auxin treatments were repeated once a week for 1 month. Seeds were collected and germinated on plates for phenotypic analysis. For *DR5::GUS* analysis, embryos were dissected from siliques 7 days after the treatment and stained with GUS staining solution.

Results

Aberrant cotyledon development in *pin1* and *pid* single mutants

A wild-type *Arabidopsis* seedling had two separated cotyledons symmetrically arranged with equal size and shape and the SAM at the center of the apex (Fig. 1A). A fraction of the *pin1* mutant seedlings displayed defects in cotyledon number, separation, position and size to various extents (Fig. 1B) (Aida et al., 2002). The frequency of cotyledon phenotype was almost equal among three strong alleles of *pin1* (Table 1). A fraction of *pid* seedlings displayed cotyledon phenotypes, similar to that of *pin1* seedlings (Fig. 1C). The *pid* mutant, however, tends to cause decrease or increase in number of cotyledons more frequently than fusion, in contrast to *pin1* in which fusion is frequently observed (data not shown). A small fraction of strong alleles, *pid-7.1.2.6* and *pid-3*, produced seedlings lacking cotyledons. The intermediate *pid-2* allele displayed slightly milder cotyledon phenotypes than did the two other *pid* alleles (Table 1). Both *pin1* and *pid* seedling phenotypes originated from embryogenesis, as evidenced by asymmetrical growth or abnormal positioning of cotyledon primordia (Fig. 1D-F) (Aida et al., 2002).

To examine in detail symmetry development as well as cotyledon primordium formation in *pin1* and *pid* mutant embryos, we analyzed the expression of marker genes that displayed specific expression patterns in the apical region of the embryo. The *AINTEGUMENTA* (*ANT*) gene was expressed in a radially symmetric ring around the embryonic apex, including cotyledon primordia at the early heart stage in wild-type embryos (Long and Barton, 1998) (Fig. 1G). *FILAMENTOUS FLOWER* (*FIL*) was expressed in the abaxial side of presumptive cotyledon primordia at the early heart stage, exhibiting bilateral symmetry (Siegfried et al., 1999) (Fig. 1H).

We analyzed the expression of these marker genes in *pin1-3*/+ or *pid-2*/+ siliques because *pin1-3* homozygous mutants were completely sterile and the fertility of *pid-2* homozygous mutants was significantly low. *ANT* was expressed in a ring in all the embryos examined in *pin1-3*/+ and *pid-2*/+ siliques (data not shown), indicating that neither homozygous mutation affected the *ANT* expression pattern. By contrast, *FIL* expression was disturbed in both *pin1-3* and *pid-2* embryos (Fig. 1I,J). In ~26% of the embryos in *pin1-3*/+ siliques (13 of 49), *FIL* was expressed in a ring that surrounded the apex of the embryos (Fig. 1I) or in an incomplete ring with a breakage at one side. *FIL* expression in a ring was detected also at the late heart stage (data not shown). In ~21% (13 out of 62) of the embryos in *pid-2*/+ siliques, *FIL* expression was asymmetric so that the strength and size of the signals differed between the two domains of expression (Fig. 1J). Taken together, the radial expression pattern of *ANT* is preserved, whereas the bilateral expression pattern of *FIL* is disturbed in *pin1* and *pid* embryos. In particular, the *pin1* mutation severely disrupts *FIL* expression, resulting in a radially symmetric pattern.

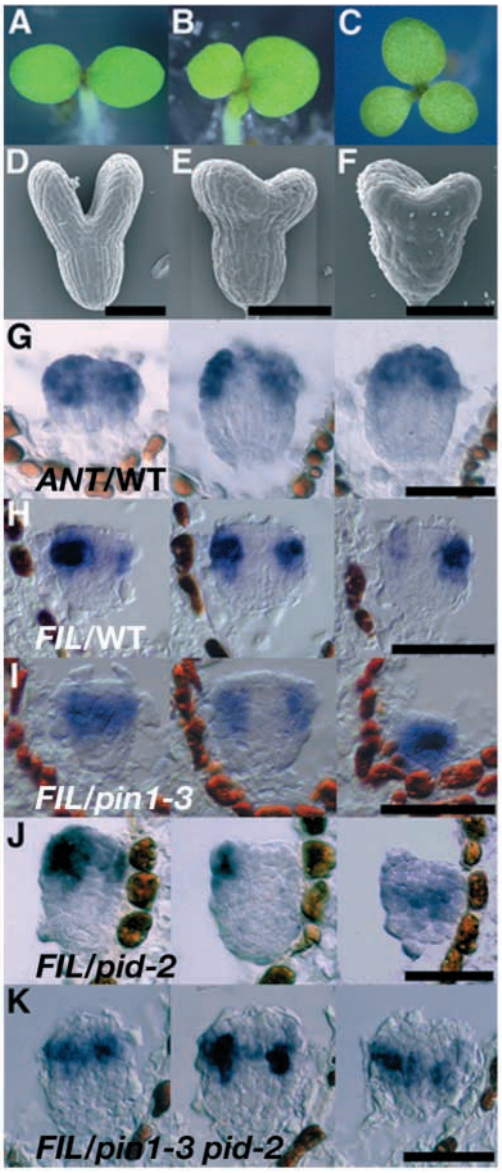

Fig. 1. Cotyledon development in wild type, *pin1* and *pid*. (A-C) Five-day-old seedlings of wild type (A), *pin1-3* (B) and *pid-2* (C). (D-F) Scanning electron micrographs of wild-type (D), *pin1-3* (E) and *pid-2* (F) embryos. (G) *ANT* expression in wild-type embryo at the early heart stage, serial longitudinal sections. (H-K) *FIL* expression in wild-type (H), *pin1-3* (I), *pid-2* (J) and *pin1-3 pid-2* (K) embryos at the early heart stage, serial longitudinal sections. Scale bars: 50 μm in D-K.

Phenotype of *pin1 pid* double mutant

To examine the genetic interaction between *PIN1* and *PID* in cotyledon development, we constructed the *pin1 pid* double mutant. Seedlings with the most severe phenotype completely lacked cotyledons, displaying radial symmetry (Fig. 2A,D; Table 2). Seedlings with the mild phenotype developed small bulges that were most likely rudimentary cotyledons. The epidermal cells of these bulges were small and round compared with those of wild-type cotyledons (Fig. 2B,E; Table 2). Seedlings that displayed the weak phenotype produced small flat structures with a ridge along the margin of the adaxial side

Table 1. Frequencies of cotyledon phenotypes

Genotype (ecotype)	Frequency of cotyledon numbers (%)				Total number of seedlings
	Zero*	One*	Two*	Three*	
pin1-3 (L*er*)	0	28.1	55.2	16.7	96
pin1-6 (WS)	0	33.9	54.8	11.3	62
pin1-201 (Col)	0	35.7	50.3	14.0	171
pid-2 (L*er*)	0	4.1	73.1	22.8	342
pid-7.1.2.6 (WS)	11.4	18.8	59.4	10.4	96
pid-3 (Col)	2.5	10.0	53.3	34.2	120

*Each category represents frequency of seedlings with corresponding numbers of separate cotyledons. In the case of fusion, one group of fused organs is counted as one cotyledon.

Table 2. Frequencies of cotyledon phenotypes in *pin1 pid* double mutants

Genotype (ecotype)	Frequency (%)			Total number of seedlings
	Severe*	Mild†	Weak‡	
pin1-3 pid-2 (L*er*)	47.3	43.6	9.1	110
pin1-6 pid-7.1.2.6 (WS)	58.3	27.8	13.9	36
pin1-201 pid-3 (Col)	58.8	20.6	20.6	34

*Seedlings completely lacking cotyledons (see Fig. 2A).
†Seedlings with small bulges (see Fig. 2B).
‡Seedlings with small flat structures having a ridge along the margin (see Fig. 2C).

(Fig. 2C; Table 2). All *pin1 pid* seedlings developed a functional SAM that produced leaf primordia, although these primordia displayed abnormal phyllotaxis and were often fused with each other (Fig. 2D, arrowheads). Mutant SAMs continued to produce leaves and eventually developed pin-like inflorescences similar to those of *pin1* or *pid* single mutant. These phenotypes were observed in three different combinations of *pin1* and *pid* alleles, including putative null mutants (Table 2; see Materials and methods). Because the observed genetic interaction was allele-nonspecific, we conclude that *PIN1* and *PID* redundantly promote cotyledon development, but are not essential for SAM formation and maintenance.

To investigate the development of cotyledon primordia and symmetry in *pin1 pid* embryos, we examined *ANT* and *FIL* expression in siliques of *pin1-3/+ pid-2/pid-2* plants as the double homozygous mutant was sterile. At the early heart stage, the expression patterns of these marker genes were almost identical to those observed in the *pin1* single mutant: *ANT* expression was normal (data not shown) and *FIL* expression formed a ring in ~19% of the embryos (seven out of 37 in *pin1-3/+ pid-2/pid-2* siliques; Fig. 1K). Similar to *pin1*, *FIL* continued to be expressed in a ring-like domain in the *pin1 pid* double mutants at the late heart stage (data not shown). Taken together, our results indicate that the *pin1 pid* double mutant fails to establish bilateral symmetry although it retains radial symmetry.

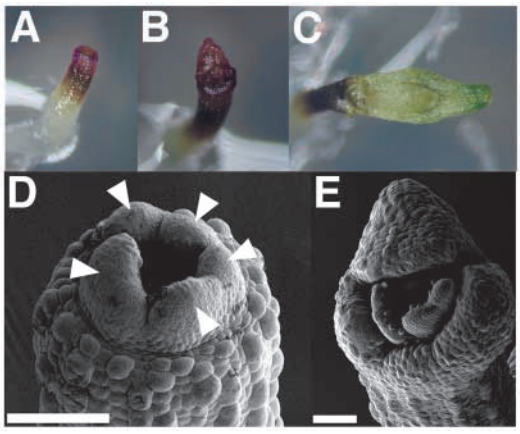

Fig. 2. Phenotype of *pin1 pid* double mutant. (A-E) Five-day-old seedlings of *pin1-3 pid-2* displaying severe (A,D), mild (B,E) and weak (C) phenotypes. (D,E) Scanning electron micrographs. Arrowheads in D indicate fused leaves with aberrant phyllotaxis. Scale bars: 100 μm in D, E.

Expression pattern of *PID*

We next examined the expression of pattern of *PID* in the embryo. Although previous studies have reported that *PID* expression is detected mainly in developing cotyledon primordia (Christensen et al., 2000; Benjamins et al., 2001), a more detailed expression study is required to assess *PID* function during embryogenesis.

At the globular stage, *PID* mRNA expression was detectable in two domains at opposite sides, each encompassing approximately three-quarters of the embryo along the longitudinal axis (Fig. 3A,H). In early heart-stage embryos, *PID* mRNA expression was again detected in two opposite domains that mainly included the boundary between cotyledon primordia and the basal part of the primordia (Fig. 3B,C,H). No expression was detected in the presumptive SAM region or at the top part of cotyledon primordia. In the late heart to torpedo stages, *PID* mRNA expression was found in the adaxial side of cotyledon primordia (Fig. 3D,H) as well as in the boundary between cotyledon primordia (Fig. 3E,H). Typically, the signal in the cotyledon boundaries was stronger than those in the other regions. Our results thus demonstrate *PID* mRNA expression at the boundaries, which has not been described in previous studies (Christensen et al., 2000; Benjamins et al., 2001).

To determine whether *PIN1* affects *PID* expression, we examined embryos developing in siliques of *pin1-3/+* plants. At the early heart stage, we found embryos in which one of the two domains of *PID* expression was significantly reduced (12 out of 57). In addition, embryos in which both expression domains were greatly reduced were found at a low frequency (five out of 57; Fig. 3F). In the late heart to torpedo stages, *PID* expression was detected in cotyledon primordia as well as in their boundaries at a level comparable with that of the wild type (Fig. 3G). These results indicate that *PID* expression partially requires *PIN1* activity at the early stage but not at the late stages.

CUC1 and *CUC2* in *pid* single and *pin1 pid* double mutants

In the wild type, the *CUC1* and *CUC2* genes, which promote cotyledon separation by preventing growth at the boundaries, were expressed in a stripe between cotyledon primordia (Fig. 4A,B). We previously have shown that, in *pin1* embryos, *CUC1* expression expands to almost the entire apex, whereas *CUC2* expression is restricted to a central spot at the early heart stage

(Aida et al., 2002). In this study, we further analyzed the expression of these genes at the late heart stage. At this stage, the expansion of *CUC1* expression to the periphery was partial, as revealed by the restricted spots of signals in cotyledon primordia (Fig. 5A). At the same stage, *CUC2* expression was mainly detected at the center of the apex and occasionally in part of the cotyledon primordia (Fig. 5B).

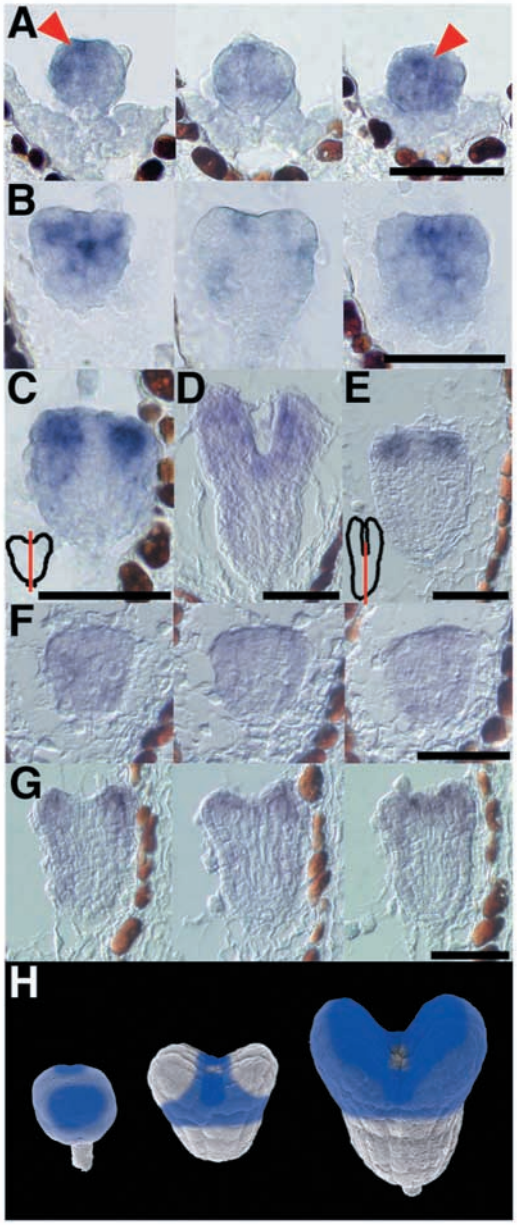

Fig. 3. *PID* mRNA expression in wild-type and *pin1* embryos. (A-E) *PID* expression in wild-type embryos at the globular stage (A) and the early heart stage (B) in serial frontal longitudinal sections; the early heart stage in sagittal longitudinal section (C), and the torpedo stage in frontal (D) and sagittal (E) sections. (F,G) Serial longitudinal sections of *pin1-3* embryo at the early heart stage (F) and the torpedo stage (G). (H) Schematic diagrams of *PID* expression in globular (left), heart (middle) and torpedo (right) stage embryos. Arrowheads in A indicate strong expression domains of *PID* mRNA. (C,E) Frontal view of each embryo with red line indicating the section plane. Scale bars: 50 μm in A-G.

We next examined the effect of *pid* mutation alone, as well as that of *pin1 pid* double mutations, on *CUC1* and *CUC2* expression. In embryos developing in *pid-2/+* siliques, we found that the stripe of *CUC1* and *CUC2* expression became slightly wide and slanted in ~10% of the transition-stage embryos (four out of 42, five out of 47 respectively; Fig. 4C,D). As cotyledon development proceeds, the expression patterns became essentially the same as that of the wild type, with a few exceptions, namely, *CUC1* expression branched into three lines or *CUC2* expression was curved, branched or broken in the middle of the stripe (data not shown). We conclude that the *pid* single mutation only mildly affects the expression of *CUC1* and *CUC2*.

To analyze *CUC1* and *CUC2* expression in the *pin1 pid* double mutant, we examined embryos developing in *pin1-3/+ pid-2/pid-2* siliques. At the early heart stage, *CUC1* expression was expanded to include nearly the entire apex in ~24% of the embryos (13 out of 55; Fig. 4E). This pattern was essentially

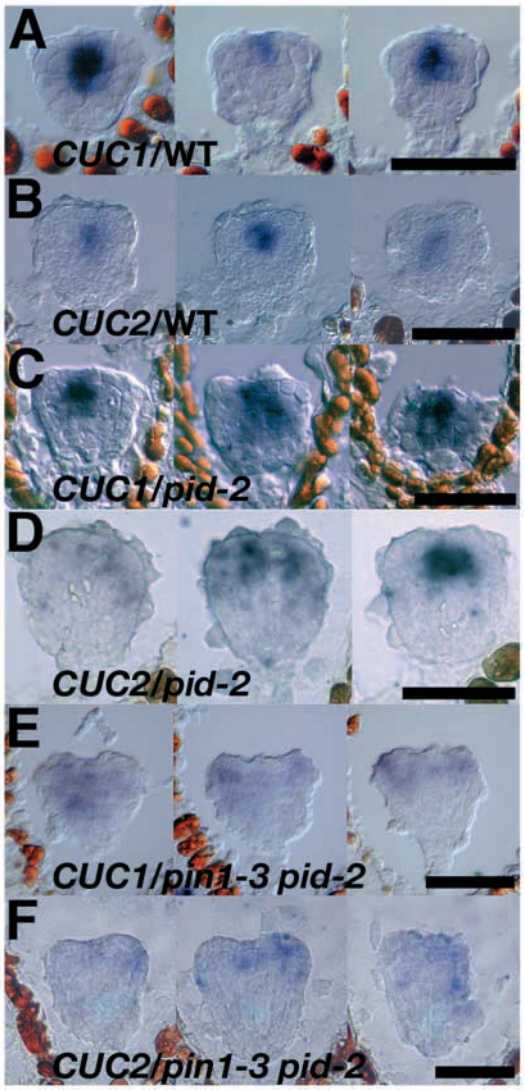

Fig. 4. Expression patterns of *CUC1* and *CUC2* in *pid* and *pin1 pid* at the early heart stage. *CUC1* (A,C,E) and *CUC2* (B,D,F) expression in serial longitudinal sections of wild-type (A,B), *pid-2* (C,D) and *pin1-3 pid-2* (E,F) embryos. Scale bars: 50 μm.

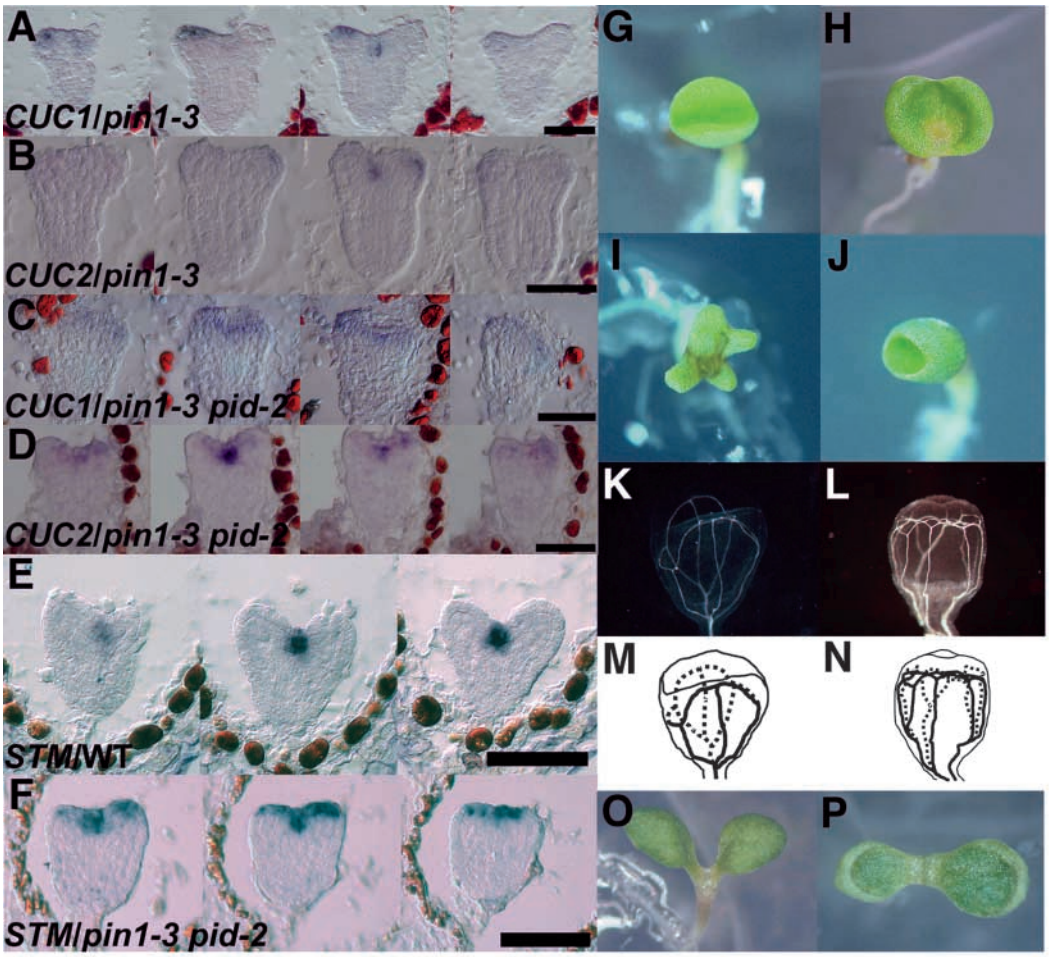

Fig. 5. Relationship between *PIN1*, *PID*, *CUC1*, *CUC2* and *STM* genes. (A-D) Expression of CUC genes in *pin1-3* (A,B) and *pin1-3 pid-2* (C,D) at the late heart stage. *CUC1* expression (A,C) and *CUC2* expression (B,D) in serial longitudinal sections. (E,F) *STM* expression in wild-type (E) and *pin1-3 pid-2* (F) embryos at the heart stage in serial longitudinal sections. (G-J,O,P) Five-day-old seedlings of *cuc1-1 cuc2* (G), *pin1-3 pid-2 cuc1-1* (H), *pin1-3 pid-2 cuc2* (I), *pin1-3 pid-2 cuc1-1 cuc2* (J), *stm-1* (O) and *pin1-3 pid-2 stm-1* (P) plants. (K,L) Seven-day-old seedlings of *cuc1-1 cuc2* (K) and *pin1-3 pid-2 cuc1-1 cuc2* (L) plants were cleared to visualize the vascular pattern. (M,N) Vascular patterns of *cuc1-1 cuc2* (M) and *pin1-3 pid-2 cuc1-1 cuc2* (N) seedlings. Scale bars: 50 μm in A-F.

the same as that in the *pin1* single mutant. At the late heart stage, however, *CUC1* expression remained in almost the entire apex of the *pin1 pid* double mutant (Fig. 5C), in contrast to that of the *pin1* single mutant. *CUC2* expression was detected in the central region and occasionally at part of the periphery in 19% of early heart stage embryos (eight out of 42; Fig. 4F). This expression pattern was maintained at the late heart stage (Fig. 5D).

Collectively, these results indicate that the *pid* mutation, when combined with *pin1*, causes a prolonged and complete expansion of *CUC1* expression into the peripheral region of the embryonic apex. This is in contrast to the *pin1* single mutant, in which the *CUC1* expression is expanded only transiently and soon becomes restricted at the late heart stage because of the action of the *PID* gene. The *pin1 pid* double mutations also cause a slight expansion of *CUC2* expression, in contrast to the *pin1* single mutation in which *CUC2* expression is reduced.

Phenotypes of *pin1 pid cuc1*, *pin1 pid cuc2* and *pin1 pid cuc1 cuc2* mutants

The prolonged expansion of *CUC1* expression as well as the slight expansion of *CUC2* expression in cotyledon primordia may account for the loss of cotyledon formation in the *pin1 pid* double mutant. To test this possibility, we constructed *pin1 pid cuc1* and *pin1 pid cuc2* triple mutants, as well as *pin1 pid cuc1 cuc2* quadruple mutant to genetically eliminate *CUC1* and/or *CUC2* function from the *pin1 pid* background.

The *pin1 pid cuc1* triple mutations markedly recovered cotyledon development, resulting in the formation of cup-shaped fused cotyledons (Fig. 5H). The extent of cotyledon fusion varied among seedlings, ranging from a partial fusion at the base to a nearly complete fusion. By contrast, most of the *pin1 pid cuc2* triple mutants were indistinguishable from the *pin1 pid* double mutants, except for a few seedlings that produced partially fused cotyledons, the sizes of which were larger than those of the rudimentary cotyledons observed in the *pin1 pid* double mutants (Fig. 5I). These results indicate that ectopic *CUC1* activity mainly prevents cotyledon formation in the *pin1 pid* double mutant and *CUC2* partially contributes to this process. The fusion phenotype observed in each triple mutant combination may be due to the reduced activities of cotyledon separation caused by the *cuc1* or *cuc2* mutation at least in part.

In the *pin1 pid cuc1 cuc2* quadruple mutant, all seedlings developed cotyledon with a fused cup shape (Fig. 5J). The extent of fusion was more pronounced and complete than that in the *pin1 pid cuc1* triple mutant. Thus, the ectopic activities of *CUC1* and *CUC2* fully account for the repression of cotyledon growth in the *pin1 pid* double mutant.

To examine symmetry in the quadruple mutant, we observed the vascular pattern of cotyledons, a suitable marker for seedling symmetry (Aida et al., 1997). Both wild-type (data not shown) and the *cuc1 cuc2* double mutant (Fig. 5G) displayed bilaterally symmetrical arrangement of vascular

strands (Fig. 5K,M). By contrast, the *pin1 pid cuc1 cuc2* quadruple mutant displays a radially symmetrical arrangement (Fig. 5L,N), similar to the arrangement described for the *pin1 cuc1 cuc2* triple mutant (Aida et al., 2002). These results are consistent with the loss of bilateral symmetry in the *pin1 pid* double mutant and indicate that the addition of *cuc1* and *cuc2* mutations does not rescue the symmetry defect.

Finally, we examined the effect of *cuc1* or *cuc2* mutation on *pid* mutation alone. In the *pid cuc1* double mutant, the extent of cotyledon fusion was slightly enhanced compared with that in the *pid* single mutant, whereas the frequency of fusion was not changed (data not shown). By contrast, seedlings of the *pid cuc2* double mutant were phenotypically indistinguishable from those of the *pid* single mutant (data not shown). These results show that neither *cuc1* nor *cuc2* markedly affects the phenotype of the *pid* single mutant.

STM expression and its activity in *pin1 pid* double mutant

We next examined the effect of the *pin1 pid* double mutations on the expression of the *STM* gene, which is involved in SAM formation and cotyledon separation downstream of the *CUC1* and *CUC2* genes (Aida et al., 1999; Takada et al., 2001). *STM* was expressed in a stripe between cotyledon primordia at the heart stage of the wild type (Fig. 5E), whereas it was expanded to include almost the entire apex in the *pin1 pid* double mutant (Fig. 5F).

To eliminate *STM* activity from the *pin1 pid* background, we constructed the *pin1 pid stm* triple mutant. Addition of the strong *stm-1* allele (Fig. 5O) to the *pin1 pid* double mutant partially recovered cotyledon development, as evidenced by the formation of large cotyledons compared with those of *pin1 pid* seedlings with mild phenotypes (Fig. 5P). The recovery of cotyledon growth by *stm*, however, was much less pronounced compared with that by the *cuc1* mutation. These results indicate that ectopic *STM* expression in the *pin1 pid* double mutant is also responsible for the growth inhibition of cotyledon primordia, although its contribution is partial.

Effects of exogenous auxin treatment on wild-type and *cuc* mutant embryos

If the observed effects of the *pin1* and *pid* mutations on the *CUC1* and *CUC2* genes were caused by changes in auxin distribution, the exogenous application of auxin could also affect these genes, thereby perturbing normal cotyledon development. Consistently, previous studies have shown that auxin treatment causes various cotyledon defects including fusion, a phenocopy of the *cuc1 cuc2* double mutant (Liu et al., 1993; Hadfi et al., 1998; Friml et al., 2003). To strengthen this hypothesis, we further tested the effect of auxin on *cuc1* and *cuc2* single mutant embryos (Materials and methods).

When wild-type embryos were treated with synthetic auxin, 2,4-dichlorophenoxyacetic acid (2,4-D), a fraction of the embryos developed into seedlings with abnormal cotyledons: 3.0% of the seedlings displayed weak fusion and 6.4% displayed complete fusion of cotyledons (Fig. 6A; Table 3). The vascular pattern of the latter class was considerably irregular and not bilaterally symmetric (Fig. 6B). In 2,4-D-treated embryos, the activity of an auxin-responsive reporter gene, *DR5::GUS* (Ulmasov et al., 1997b; Sabatini et al., 1999; Friml et al., 2003), was detected in a broader region compared with that in mock-treated embryos (Fig. 6C,D). These results suggest that the application of auxin to the embryo changes the auxin distribution in the apical region and causes cotyledon fusion, possibly by reducing the activities of the CUC genes.

We next treated *cuc1* and *cuc2* single mutant embryos with 2,4-D. Interestingly, auxin treatment of the *cuc1* single mutant resulted in a significantly higher frequency of seedlings with the strong fusion phenotype (Table 3) than that of the wild type. However, the effect of auxin on the *cuc2* single mutant was similar to that on the wild type (Table 3). Considering that neither *cuc1* nor *cuc2* mutation changes auxin sensitivity per se (Daimon et al., 2003) and that the *CUC1* and *CUC2* genes are functionally redundant (Aida et al., 1997), the observed higher frequency of the fusion phenotype in *cuc1* embryos may suggest that the activity of *CUC2* is reduced more effectively than that of *CUC1* upon auxin application.

Discussion

In this study, we demonstrated a synergistic interaction between mutations in the *PIN1* and *PID* genes, the functions of which are implicated in auxin-mediated organ formation.

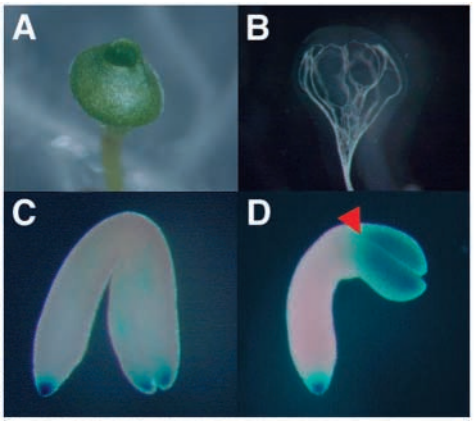

Fig. 6. Effects of treatment with exogenous auxin on embryo. (A,B) Five-day-old seedlings treated with 2,4-D during embryogenesis. In B, the seedling was cleared to visualize the vascular pattern. (C,D) Spatial expression pattern of *DR5::GUS* in mature embryos. Mock (C) and 2,4-D (D) treatment. The fused part of cotyledons is indicated by a red arrowhead in D.

Table 3. Effects of auxin treatment on embryogenesis

Genotype	Frequency (%)			Total number of seedlings
	Cup-shaped*	Partial fusion†	Normal	
L*er*	–	–	–	–
cuc1-1‡	0	0.5	99.5	–
cuc2‡	0	0.5	99.5	–
L*er*+2,4-D	6.4	3.0	90.6	202
cuc1-1+2,4-D	28.3	4.2	67.5	166
cuc2+2,4-D	3.0	7.4	89.6	230

*Cotyledons are completely fused and surround the entire apex.
†Cotyledons are partially fused at the base.
‡Taken from Aida et al. (Aida et al., 1997).

Seedlings of the *pin1* and *pid* single mutants exhibited relatively mild defects in cotyledon development, whereas those of the double mutant completely lacked cotyledons in the most severe cases. The synergistic interaction between *pin1* and *pid* mutations was not specific to the combination of alleles, suggesting that the *PIN1* and *PID* genes act redundantly in the same process. Our results illustrate two major aspects of *PIN1* and *PID* functions in embryogenesis: establishment of bilateral symmetry and promotion of cotyledon growth.

PIN1 and *PID* function in apical patterning of cotyledon primordia and their boundaries

The apical region of the embryo can be divided into three subregions, each of which follows different developmental fates (Fig. 7A) (Aida et al., 1999). In the wild type, *CUC1* and *CUC2* are expressed in both the presumptive SAM (PS) and the boundary of cotyledon margins (BCM), whereas *FIL* is expressed in the cotyledon primordia (CP). The expression patterns of these three genes are bilaterally symmetric. By contrast, *ANT* is expressed in both CP and BCM, reflecting radial symmetry. The single and double mutants of *pin1* and *pid* all develop a functional SAM, suggesting that *PIN1* and *PID* are not essential for the establishment of PS. Consistent with this, none of the expressions of the above markers reveal any abnormalities in PS of the *pin1* and *pid* mutants.

The expression patterns of the bilateral markers indicate that *PIN1* and *PID* regulate patterning in the peripheral region consisting of CP and BCM. At the early heart stage, both *CUC1* and *FIL* are expressed as a ring in the peripheral region of *pin1*, suggesting that this region has a mixed identity of CP and BCM (Fig. 7B) and that *PIN1* is essential for the initial positioning and partitioning of CP and BCM within the peripheral region. By contrast, no or only partial overlap of CP and BCM seems to occur in *pid* embryos, as reflected by relatively mild change of *CUC1*, *CUC2* and *FIL* expression patterns in *pid-2* embryos. This finding may suggest that *PID* is not involved in the peripheral patterning process at the early heart stage. Alternatively, *PID* may be required for this process but the effect of *pid-2* mutation is not apparent, simply because of the residual *PID* activity in this intermediate allele.

As embryogenesis proceeds, the area of BCM becomes partially excluded from CP in the *pin1* single mutant (Fig. 7C), as indicated by the partial exclusion of the ectopic *CUC1* expression at the late heart stage. This exclusion is dependent on *PID*, as the ectopic *CUC1* expression remains in the entire peripheral region in the *pin1 pid* background at the same stage (Fig. 7D). This finding indicates that the late activity of *PID* can partially compensate for the failure caused by the loss of *PIN1* activity.

Analysis of the *pin1*and *pid* mutants in the inflorescence meristem has suggested a difference between the functions of these genes (Reinhardt et al., 2003). When a large amount of auxin is applied locally to the inflorescence meristem of *pin1*, a fused, color-like flower primordium is induced at a site close to the application. By contrast, the same amount of auxin applied to the *pid* meristem induces multiple primordia having a normal size but no fusion. The observed response of *pin1* meristems is consistent with the idea that *PIN1* is involved in organ partitioning in both the embryo and the inflorescence meristem. However, the response of *pid* inflorescence meristems does not reveal any involvement of the *PID* gene in flower primordium partitioning, in contrast to its proposed function based on our analysis of embryogenesis. This difference may reflect different functions of the *PID* gene between embryo and flower development. Alternatively, *pid* inflorescence meristems may also display partitioning defects that can be detected only by molecular markers during the early stages of primordium formation.

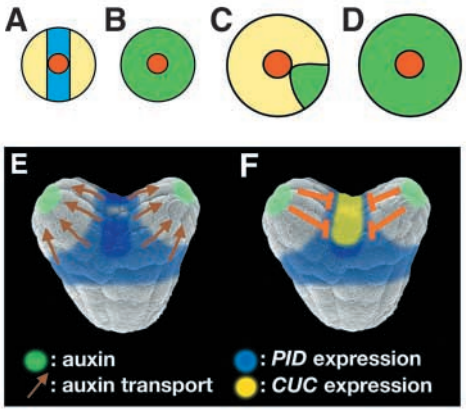

Fig. 7. Apical patterning during embryogenesis. (A-D) Mutant phenotypes. (A,B) Apical region of the early-heart stage embryo. (A) Wild-type apex is divided into three subregions, presumptive SAM (PS; orange), cotyledon primordia (CP; yellow) and boundary of cotyledon margins (BCM; blue). (B) In the *pin1-3* or *pin1-3 pid-2* embryo, the peripheral region possesses a mixed identity of CP and BCM, which is shown in green. (C,D) Late heart stage. The area of BCM is reduced in *pin1-3* (C), while the entire peripheral region continues to express a mixed identity of CP and BCM in *pin1-3 pid-2* (D). (E,F) Model for apical patterning during embryogenesis. (E) *PID* expression (blue) accumulates mainly in the boundaries of cotyledon primordia and slightly in regions that surround the base of cotyledon primordia. *PIN1* and *PID* redundantly promote auxin transport toward the tips of the cotyledon primordia (brown arrows), resulting in the formation of auxin gradient maxima (green). (F) Auxin accumulation in cotyledon primordia (green) prevents CUC gene expression (yellow) from expanding to the periphery.

PIN1 and *PID* promote cotyledon growth by repressing *CUC1*, *CUC2* and *STM* activities

The prolonged expansion of *CUC1* and *CUC2* expression in the apex of the *pin1 pid* embryos suggests that cotyledon growth is suppressed by the ectopic activities of these genes. The elimination of both *CUC1* and *CUC2* activities from *pin1 pid* (i.e. quadruple mutant) results in the complete recovery of cotyledon growth, as evidenced by a fused cup-shaped cotyledon that surrounds the seedling apex. These results indicate that *PIN1* and *PID* function to repress *CUC1* and *CUC2* expression and/or activity in cotyledon primordia, thereby allowing the primordia to develop. In contrast to the *pin1 pid* double mutant, the *pin1* single mutant does not display severe reduction in cotyledon growth, despite the expansion of *CUC1* expression. This is probably because that the expansion of *CUC1* occurs only transiently. The later exclusion of *CUC1* expression from the peripheral region may be sufficient for the primordia to develop fully.

Although the *pin1 pid* embryos display severe reduction or complete loss of cotyledon growth, they express both *ANT* and

FIL, each of which promotes different aspects of shoot organ development (Long and Barton, 1998; Sawa et al., 1999; Siegfried et al., 1999). This observation suggests that the double mutant initiates developmental programs for cotyledon development at least in part. This notion is consistent with the recovery of cotyledon growth in the *pin1 pid cuc* triple and quadruple mutants, which indicates that the embryos are competent to form cotyledons even when both *PIN1* and *PID* activities are reduced.

The expression patterns of marker genes have also been examined in the inflorescence meristem of the *pin1* mutant (Vernoux et al., 2000). Similar to the embryo, the expression of primordium-specific genes such as *LFY* and *ANT* is still present, and their expression domains overlap with that of the boundary-specific *CUC2* gene, again suggesting that *pin1* maintains competence for primordium growth although the growth is suppressed by the ectopic expression of boundary specific factors. Taken together, these results indicate that *PIN1* and *PID* promote shoot organ growth by repressing negative factors for organ formation such as the *CUC1*, *CUC2* and *STM* genes, rather than promoting positive factors, in both the embryo and the inflorescence meristem.

Auxin and apical patterning of embryo

Recent studies have shown that an auxin gradient maximum is present in initiating organ primordia (Benková et al., 2003; Friml et al., 2003). In the embryo, the maxima of auxin gradients are present at the tips of cotyledon and root primordia, and those at the cotyledon primordia are likely to be dependent mainly on PIN1, although other members of the PIN family are also suggested to have partially redundant functions (Benková et al., 2003) (Fig. 7E). Complementary distributions of the auxin gradient maxima and the domain of *CUC1* and *CUC2* expression suggest that auxin negatively regulates the expression of these genes (Fig. 7F). This idea is consistent with our auxin application experiment, showing that an increased concentration of auxin in the apical region induces the cotyledon fusion phenotype. The frequency of the phenotype is higher in the *cuc1* mutant than in the *cuc2* mutant. Because each mutation does not affect auxin response per se (Daimon et al., 2003), this result may suggest that *CUC2* is more effectively repressed by auxin than is *CUC1*.

Our results demonstrate that *PID* has an overlapping function with *PIN1* in patterning the periphery of the embryonic apex. *PID* transcripts accumulate mainly at the boundaries of cotyledon primordia and slightly in regions that surround the base of cotyledon primordia (Fig. 7E). We also found that *PID* expression at the early heart stage is dependent on *PIN1*. Considering that *PID* is an auxin-inducible gene (Benjamin et al., 2001), we speculate that the initial *PID* expression is induced in response to the auxin distribution established by *PIN1*. Although the precise cellular function of the PID protein is still unclear, previous studies have suggested its role in promoting auxin transport (Benjamin et al., 2001). As *PID* and CUC expression domains are overlapping in the boundary of cotyledon primordia, we suggest that *PID*, by promoting auxin transport, reduces the level of auxin at the boundary and increases it in the primordia (Fig. 7E) to limit *CUC1* and *CUC2* expression to the boundary (Fig. 7F). Detailed analysis of the effects of *PID* on auxin transport and distribution and identification of the cellular process in which *PID* functions are required for uncovering the mechanism by which *PID* regulates patterning in the apical region of the embryo.

We thank Miyo Terao Morita for critical reading of the manuscript. We also thank David R. Smyth for providing *pid-2* and *pid-3* seeds. This work was partially supported by Grants-in-Aid for Scientific Research on Priority Areas from the Ministry of Education, Science, and Culture, Sports, Science, and Technology of Japan (14036222 to M.T.) and Encouragement of Young Scientists (12740439 to M.A.). M.F. was supported by fellowships from the Japan Society for the Promotion of Science.

References

Aida, M., Ishida, T., Fukaki, H., Fujisawa, H. and Tasaka, M. (1997). Genes involved in organ separation in Arabidopsis: an analysis of the *cup-shaped cotyledon* mutant. *Plant Cell* **9**, 841-857.

Aida, M., Ishida, T. and Tasaka, M. (1999). Shoot apical meristem and cotyledon formation during Arabidopsis embryogenesis: interaction among the CUP-SHAPED COTYLEDON and SHOOT MERISTEMLESS genes. *Development* **126**, 1563-1570.

Aida, M., Vernoux, T., Furutani, M., Traas, J. and Tasaka, M. (2002). Roles of PIN-FORMED1 and MONOPTEROS in pattern formation of the apical region of the Arabidopsis embryo. *Development* **129**, 3965-3974.

Alonso, J. M., Stepanova, A. N., Leisse, T. J., Kim, C. J., Chen, H., Shinn, P., Stevenson, D. K., Zimmerman, J., Barajas, P., Cheuk, R. et al. (2003). Genome-wide insertional mutagenesis of Arabidopsis thaliana. *Science* **301**, 653-657.

Barton, M. K. and Poethig, R. S. (1993). Formation of the shoot apical meristem in Arabidopsis thaliana: an analysis of development in the wild type and in the shoot meristemless mutant. *Development* **119**, 823-831.

Benjamins, R., Quint, A., Weijers, D., Hooykaas, P. and Offringa, R. (2001). The PINOID protein kinase regulates organ development in Arabidopsis by enhancing polar auxin transport. *Development* **128**, 4057-4067.

Benková, E., Michniewicz, M., Sauer, M., Teichmann, T., Seifertová, D., Jürgens, G. and Friml, J. (2003). Local, efflux-dependent auxin gradients as a common module for plant organ formation. *Cell* **115**, 591-602.

Bennett, S. R. M., Alvarez, J., Bossinger, G. and Smyth, D. R. (1995). Morphogenesis in pinoid mutants of Arabidopsis thaliana. *Plant J.* **8**, 505-520.

Berleth, T. and Jürgens, G. (1993). The role of the monopteros gene in organising the basal body region of the Arabidopsis embryo. *Development* **118**, 575-587.

Bowman, J. L. and Eshed, Y. (2000). Formation and maintenance of the shoot apical meristem. *Trends Plant Sci.* **5**, 110-115.

Christensen, S. K., Dagenais, N., Chory, J. and Weigel, D. (2000). Regulation of auxin response by the protein kinase PINOID. *Cell* **100**, 469-478.

Clark, S. E., Jacobsen, S. E., Levin, J. Z. and Meyerowitz, E. M. (1996). The CLAVATA and SHOOT MERISTEMLESS loci competitively regulate meristem activity in Arabidopsis. *Development* **122**, 1567-1575.

Daimon, Y., Takabe, K. and Tasaka, M. (2003). The CUP-SHAPED COTYLEDON genes promote adventitious shoot formation on calli. *Plant Cell Physiol.* **44**, 113-121.

Endrizzi, K., Moussian, B., Haecker, A., Levin, J. Z. and Laux, T. (1996). The SHOOT MERISTEMLESS gene is required for maintenance of undifferentiated cells in Arabidopsis shoot and floral meristem and acts at a different regulatory level than the meristem genes WUSCHEL and ZWILLE. *Plant J.* **10**, 967-979.

Friml, J., Benková, E., Blilou, I., Wisniewska, J., Hamann, T., Ljung, K., Woody, S., Sandberg, G., Scheres, B., Jürgens, G. and Palme, K. (2002). AtPIN4 mediates sink-driven auxin gradients and root patterning in Arabidopsis. *Cell* **108**, 661-673.

Friml, J., Vieten, A., Sauer, M., Weijers, D., Schwarz, H., Hamann, T., Offringa, R. and Jürgens, G. (2003). Efflux-dependent auxin gradients establish the apical-basal axis of Arabidopsis. *Nature* **426**, 147-153.

Fukaki, H., Fujisawa, H. and Tasaka, M. (1996). Gravitropic response of inflorescence stems in Arabidopsis thaliana. *Plant Physiol.* **110**, 933-943.

Furutani, M., Aida, M. and Tasaka, M. (2003). Pattern formation during dicotyledonous plant embryogenesis. In *Morphogenesis and Pattern*

Formation in Biological Systems (ed. T. Sekimura, S. Noji and P. K. Maini), pp. 139-152. Tokyo: Springer-Verlag.

Gälweiler, L., Guan, C., Müller, A., Wisman, E., Mendgen, K., Yephremov, A. and Palme, K. (1998). Regulation of polar auxin transport by AtPIN1 in Arabidopsis vascular tissue. *Science* **282**, 2226-2230.

Hadfi, K., Speth, V. and Neuhaus, G. (1998). Auxin-induced developmental patterns in Brassica juncea embryos. *Development* **125**, 879-887.

Hardtke, C. S. and Berleth, T. (1998). The Arabidopsis gene MONOPTEROS encodes a transcription factor mediating embryo axis formation and vascular development. *EMBO J.* **17**, 1405-1411.

Jürgens, G. (2001). Apical-basal pattern formation in Arabidopsis embryogenesis. *EMBO J.* **20**, 3609-3616.

Jürgens, G. and Mayer, U. (1994). Arabidopsis. In *Embryos: Colour Atlas of Development* (ed. J. Bard), pp. 7-21. London: Wolfe.

Liu, C., Xu, Z. and Chua, N.-H. (1993). Auxin polar transport is essential for the establishment of bilateral symmetry during early plant embryogenesis. *Plant Cell* **5**, 621-630.

Long, J. A. and Barton, M. K. (1998). The development of apical embryonic pattern in Arabidopsis. *Development* **125**, 3027-3035.

Long, J. A., Moan, E. I., Medford, J. I. and Barton, M. K. (1996). A member of the KNOTTED class of homeodomain proteins encoded by the STM gene of Arabidopsis. *Nature* **379**, 66-69.

Okada, K., Ueda, J., Komaki, M. K., Bell, C. J. and Shimura, Y. (1991). Requirement of the auxin polar transport system in early stages of Arabidopsis floral bud formation. *Plant Cell* **3**, 677-684.

Reinhardt, D., Pesce, E., Stieger, P., Mandel, T., Baltensperger, K., Bennett, M., Traas, J., Friml, J. and Kuhlemeier, C. (2003). Regulation of phyllotaxis by polar auxin transport. *Nature* **426**, 255-260.

Sabatini, S., Beis, D., Wolkenfelt, H., Murfett, J., Guilfoyle, T., Malamy, J., Benfey, P., Leyser, O., Bechtold, N., Weisbeek, P. and Scheres, B. (1999). An auxin-dependent distal organizer of pattern and polarity in the Arabidopsis root. *Cell* **99**, 463-472.

Sawa, S., Watanabe, K., Goto, K., Kanaya, E., Morita, E. H. and Okada, K. (1999). FILAMENTOUS FLOWER, a meristem and organ identity gene of Arabidopsis, encodes a protein with a zinc finger and HMG-related domains. *Genes Dev.* **13**, 1079-1088.

Siegfried, K. R., Eshed, Y., Baum, S. F., Otsuga, D., Drews, G. N. and Bowman, J. L. (1999). Members of the YABBY gene family specify abaxial cell fate in Arabidopsis. *Development* **126**, 4117-4128.

Takada, S., Hibara, K., Ishida, T. and Tasaka, M. (2001). The CUP-SHAPED COTYLEDON1 gene of Arabidopsis regulates shoot apical meristem formation. *Development* **128**, 1127-1135.

Ulmasov, T., Hagen, G. and Guilfoyle, T. J. (1997a). ARF1, a transcription factor that binds to auxin response elements. *Science* **276**, 1865-1868.

Ulmasov, T., Murfett, J., Hagen, G. and Guilfoyle, T. J. (1997b). Aux/IAA proteins repress expression of reporter genes containing natural and highly active synthetic auxin response elements. *Plant Cell* **9**, 1963-1971.

Vernoux, T., Kronenberger, J., Grandjean, O., Laufs, P. and Traas, J. (2000). PIN-FORMED 1 regulates cell fate at the periphery of the shoot apical meristem. *Development* **127**, 5157-5165.